

Role of standing-wave mode structure in microlaser emission

Kyungwon An and Michael S. Feld

George R. Harrison Spectroscopy Laboratory, Massachusetts Institute of Technology, Cambridge, Massachusetts 02139

(Received 1 February 1995)

In the recently developed microlaser, a single two-level atom interacts with a single mode of the optical resonator to generate coherent radiation. The resonator mode is in the form of a standing wave. We present an analysis of the standing-wave features, based on an approximate solution of the fully quantized microlaser equations. The result explains the rapid increase in the observed signal when the average number of atoms in the cavity is of the order of 1.

PACS number(s): 42.50.-p, 42.55.-f

I. INTRODUCTION

The recent development of the microlaser [1] has opened up important new possibilities in the field of cavity quantum electrodynamics [2,3]. In this experiment, inverted two-level atoms in an atomic beam traversing an ultrahigh Q optical resonator interact with the cavity mode one by one and emit photons into the resonator. Because of the long cavity storage time, a large number of photons can build up. The microlaser is the optical analog of the micromaser [4,5], which operates in the microwave regime. In both devices the photon generation process follows the Jaynes-Cummings model [6]. However, operation in the optical range provides new experimental opportunities associated with the large increases in photon energy and momentum. The increase in photon energy allows measurement of the microlaser mean photon number and emission spectrum [7-10] via direct photon detection, whereas only atoms can be probed in the micromaser. The increased photon momentum should make it possible to study the entanglement of the quantized Rabi oscillations with the mechanical degrees of freedom of the atom, as exchange of a single optical photon with the cavity field can significantly deflect the atomic trajectory. In addition, the absence of blackbody radiation at optical frequencies opens the possibility of studying the features of quantum collapse and revival [11], which are entirely due to the superposition of discrete photon-number Fock states in the cavity field. Also promising is the possibility of generating and studying photon-number trapped states [12,13].

This paper is a follow-up to Ref. [1], intended to provide details about how we obtained the theoretical predictions that were compared with experiment. The microlaser experiment in Ref. [1] studied the mean photon number in the cavity $\langle n \rangle$ as a function of the average number of atoms $\langle N \rangle$ present there. For $\langle N \rangle \ll 1$ the results were found to agree with the predictions of the fully quantized single-atom microlaser theory. However, at about $\langle N \rangle \simeq 0.6$ a rapid increase in $\langle n \rangle$, not predicted by the theory, was observed, and as $\langle N \rangle$ approached unity, $\langle n \rangle$ was found to be anomalously large. This deviation, we believe, is caused by two effects: the breakdown of the one-atom theory and the standing-wave

mode structure of the cavity combined with the saturation effect for large $\langle n \rangle$. Note that the one-atom quantum theory is not valid when $\langle N \rangle$ approaches unity; because of the Poissonian distribution of the number of atoms, the probability of having two or three atoms in the cavity is then comparable to that of having only one atom present. In addition, there exists a second effect that can also increase $\langle n \rangle$, even when, for example, $\langle N \rangle \simeq 0.6$, for which the single-atom assumption is probably not significantly violated (the probability for more than one atom is 13% compared to 26% when $\langle N \rangle = 1$). This effect is associated with the standing-wave nature of the optical resonator mode. The standing-wave spatial dependence directly reflects itself in the spatial dependence of the atom-cavity coupling and can have a profound effect on the number of photons in the cavity mode. As shown below, this feature, coupled with the saturation of the atom-field interaction for large $\langle n \rangle$, can explain the observed rapid increase in $\langle n \rangle$ near $\langle N \rangle \simeq 0.6$.

II. MICROLASER THEORY

In the microlaser experiment of Ref. [1], the atoms were prepared by passing the atomic beam through an excitation laser beam just before they entered the cavity. The intensity and the waist of this laser beam were adjusted so that atoms entering the cavity with the most probable velocity experienced a π pulse, exciting them to a state of complete inversion. However, due to the broad thermal velocity distribution of the atomic beam, a significant portion of the atoms as not completely inverted and entered the cavity in superposition states. In order to properly describe the resulting photon buildup, the micromaser theory of Ref. [5] must be modified to include this feature.

The interaction of a single two-level atom with a single cavity mode can be described by the Jaynes-Cummings Hamiltonian, given by

$$H = \frac{1}{2} \hbar \omega_a S_z + \hbar \omega a^\dagger a + \hbar g (S_+ a + S_- a^\dagger) . \quad (1)$$

Here g is the atom-field coupling constant, given by

$$g = \frac{\mu}{\hbar} \sqrt{\frac{2\pi\hbar\omega}{V_m}}, \quad (2)$$

with V_m the mode volume of the cavity; ω_a the atomic transition frequency; a^\dagger and a the creation and the annihilation operator for the photons in the field mode, respectively; and S_+ , S_- , and S_z the Pauli spin matrices. When no atom is present in the cavity, the field density operator ρ^F undergoes decay due to cavity damping. Since the number of photons associated with blackbody

radiation even at room temperature is virtually zero in the microlaser ($n_b = 10^{-28}$), the equation of motion is then simply

$$\frac{d\rho^F}{dt} = \frac{\Gamma_c}{2} (2a\rho^F a^\dagger - a^\dagger a\rho^F - \rho^F a^\dagger a), \quad (3)$$

with Γ_c the cavity damping rate. If an atom enters the cavity at $t = 0$ and exits at $t = t_{\text{int}}$, the field density matrix elements at time t , $0 < t < t_{\text{int}}$, can be shown to satisfy the recursion relation

$$\begin{aligned} \rho_{n,m}^F(t) = & \rho_{n,m}^F(0) \{ \rho_{aa}^A [C_n(t)C_m(t) + S_n^\delta(t)S_m^\delta(t) - i [C_n(t)S_m^\delta(t) - C_m(t)S_n^\delta(t)]] \} \\ & + \rho_{bb}^A \{ C_{n-1}(t)C_{m-1}(t) + S_{n-1}^\delta(t)S_{m-1}^\delta(t) + i [C_{n-1}(t)S_{m-1}^\delta(t) - C_{m-1}(t)S_{n-1}^\delta(t)] \} \\ & + \rho_{n+1,m+1}^F(0) \rho_{bb}^A S_n^\kappa(t) S_m^\kappa(t) + \rho_{n-1,m-1}^F(0) \rho_{aa}^A S_{n-1}^\kappa(t) S_{m-1}^\kappa(t) \\ & + i \rho_{n,m+1}^F(0) \rho_{ab}^A [C_n(t) + iS_n^\delta(t)] S_m^\kappa(t) - i \rho_{n+1,m}^F(0) \rho_{ba}^A S_n^\kappa(t) [C_m(t) - iS_m^\delta(t)] \\ & + i \rho_{n,m-1}^F(0) \rho_{ba}^A [C_{n-1}(t) - iS_{n-1}^\delta(t)] S_{m-1}^\kappa(t) - i \rho_{n-1,m}^F(0) \rho_{ab}^A S_{n-1}^\kappa(t) [C_{m-1}(t) + iS_{m-1}^\delta(t)], \end{aligned} \quad (4)$$

where

$$\rho_{xy}^A \equiv c_x(0)c_y^*(0), \quad x, y = a, b \quad (5a)$$

$$C_n = \cos \left[\frac{1}{2} \sqrt{\kappa_n^2 + \Delta^2} t \right], \quad (5b)$$

$$S_n^\delta = \frac{\Delta}{\sqrt{\kappa_n^2 + \Delta^2}} \sin \left[\frac{1}{2} \sqrt{\kappa_n^2 + \Delta^2} t \right], \quad (5c)$$

$$S_n^\kappa = \frac{\kappa_n}{\sqrt{\kappa_n^2 + \Delta^2}} \sin \left[\frac{1}{2} \sqrt{\kappa_n^2 + \Delta^2} t \right], \quad (5d)$$

$$\kappa_n = 2g\sqrt{n+1}, \quad (5e)$$

with $c_a(t)$ and $c_b(t)$ the probability amplitudes of the atom in the upper and lower states, respectively, and Δ the atom-cavity frequency detuning. When no atom is present in the resonator mode (i.e., for $t > t_{\text{int}}$), the field decays to zero according to Eq. (3). In terms of the

elements of the density matrix, this equation becomes

$$\begin{aligned} \frac{d\rho_{n,m}^F}{dt} = & \Gamma_c \left[\sqrt{(n+1)(m+1)} \rho_{n+1,m+1}^F \right. \\ & \left. - \frac{1}{2}(n+m) \rho_{n,m}^F \right]. \end{aligned} \quad (6)$$

Equations (4) and (6) provide a general description of the microlaser.

We next derive a recursion relation combining Eqs. (4) and (6). Details of the derivation are presented in the Appendix. In short, we employ the recipe of Ref. [5] to perform an average over the random arrival times of atoms entering the cavity and then invoke the boundary condition that the field density matrix repeats the same time evolution for every atom, once an equilibrium is reached. Denoting the field density matrix elements in the equilibrium state by $Q_{n,m}$ after averaging over random arrival times with mean time interval Δt , we find a reduced recursion relation

$$\begin{aligned} \left[1 + \frac{1}{2} \Gamma_c \Delta t (n+m) \right] Q_{n,m} = & Q_{n,m} \{ N_a [C_n C_m + S_n^\delta S_m^\delta - i (C_n S_m^\delta - C_m S_n^\delta)] \\ & + (1 - N_a) [C_{n-1} C_{m-1} + S_{n-1}^\delta S_{m-1}^\delta + i (C_{n-1} S_{m-1}^\delta - C_{m-1} S_{n-1}^\delta)] \} \\ & + Q_{n+1,m+1} \left[(1 - N_a) S_n^\kappa S_m^\kappa + \Gamma_c \Delta t \sqrt{(n+1)(m+1)} \right] + Q_{n-1,m-1} N_a S_{n-1}^\kappa S_{m-1}^\kappa \\ & + [Q_{n,m-1} (C_{n-1} - iS_{n-1}^\delta) S_{m-1}^\kappa + Q_{n-1,m} S_{n-1}^\kappa (C_{m-1} + iS_{m-1}^\delta) \\ & - Q_{n,m+1} (C_n + iS_n^\delta) S_m^\kappa - Q_{n+1,m} S_n^\kappa (C_m - iS_m^\delta)] \sqrt{N_a(1 - N_a)}, \end{aligned} \quad (7)$$

where N_a is the probability that the atom is in the excited state when it enters the cavity and C_n, S_n^κ , and S_n^δ are evaluated at $t = t_{\text{int}}$. Note that $Q_{n,m}$ is coupled to all of its nearest neighbors except $Q_{n-1,m+1}$ and $Q_{n+1,m-1}$. Once the field density matrix elements in the equilibrium state are evaluated using Eq. (7), $\langle n \rangle$ can be calculated from

$$\langle n \rangle = \int_0^\infty dv f_B(v) \sum_{k=1}^\infty k Q_{k,k}(v), \quad (8)$$

with $f_B(v)$ the Maxwell-Boltzmann velocity distribution function.

When the atoms are prepared in a superposition state, even if we start from a vacuum state ($Q_{0,0} = 1$), eventually all of the matrix elements become excited. Suppose that the first atom enters the cavity at $t = 0$. According to Eq. (7), just after the first atom-field interaction not only $Q_{1,1}$ and $Q_{0,0}$ but also $Q_{1,0}$ and $Q_{0,1}$ become nonzero. An interaction with a second atom will then excite any $Q_{n,m}$ with $n, m = 0, 1, 2$. In general, all the $Q_{n,m}$ components with $n, m = 0, 1, \dots, k$ become excited after an interaction with the k th atom. This growth eventually tapers off due to cavity decay.

III. EFFECTS OF THE STANDING-WAVE RESONATOR MODE

We now consider the spatial dependence of the atom-field coupling within the cavity. In the micromaser it is reasonable to assume that this coupling is spatially uniform since a low-order standing-wave mode of the cavity is excited. Low order implies a cavity mode in which a few integer multiples of a half wavelength fit into the cavity. Since the wavelength is of the order of a few centimeters, it is relatively easy to align the atomic beam along the antinode of the cavity mode, ensuring that all the atoms have the same coupling constant. In contrast, the microlaser employs an open optical resonator with high-order standing-wave modes. Typically 10^3 – 10^4 wavelengths can fit into the cavity. Since the diameter of the atomic beam is typically much larger than the wavelength, the atom-field coupling constant varies sinusoidally along its width. In addition, since the cavity mode has a Gaussian field distribution in the transverse direction, the coupling constant also varies accordingly. Therefore, the coupling constant g appearing in Eq. (4) via C_n, S_n^κ , and S_n^δ becomes a function of the position \vec{r} of the atom:

$$g(\vec{r}) = g_0 \exp\left[-\frac{x^2 + y^2}{w_m^2}\right] \cos kz, \quad (9)$$

in which g_0 is given by

$$g_0 = \frac{\mu}{\hbar} \sqrt{\frac{2\pi\hbar\omega}{V_m}}, \quad (10)$$

with z the position of the atom along the axis of the resonator and x and y the transverse coordinates, with

the beam of atoms moving along the x axis. In Eq. (9), w_m is the waist of the cavity mode and $\cos kz$ accounts for its standing-wave spatial variation.

It may appear that the position dependence of the coupling constant can be taken into account by solving the recursion relation for $Q_{n,m}$ and then simply averaging over the distributions of y and z (variation in x is handled by t_{int} , which is independent of y and z). This averaging scheme is correct only if the interaction between an atom and the field is independent of the interactions among the preceding atoms and the field. However, in the present case one event of the atom-field interaction is not independent of the preceding events. The cavity field, which is the result of all preceding atom-field interactions, does not decay appreciably by the time the next atom arrives and so influences the subsequent atom-field interaction.

In order to see that the post-averaging scheme is incorrect, consider a pair of infinitely narrow atomic beams of equal flux, both propagating parallel to the x axis in the $y=0$ plane. One beam, labeled A , passes through the field mode at a node ($\cos^2 kz = 0$) of the cavity; the other, labeled B , passes through an antinode ($\cos^2 kz = 1$). Note that the atoms passing through the node do not couple to the cavity field and thus do not contribute to photon buildup in the cavity. In contrast, the atoms passing through the antinode interact with the field with the full magnitude of the coupling constant g_0 . Assume that atoms from the two beams enter the cavity alternately, with Δt_{whole} the average time interval between the arrival of successive atoms, one from beam A followed by one from beam B . The mean time interval between successive arrivals from a single beam is $2\Delta t_{\text{whole}}$. The post-averaging scheme then results in an average of two configurations: atoms traversing either the antinode or the node, each with 50% probability. Since the atomic beam intersecting the node does not interact, this averaging scheme gives a mean photon number that is just half of the mean photon number that would be obtained from a single beam traversing the antinode of the cavity with the mean time interval Δt_{whole} between arriving atoms. Note that this is not the same as the correct mean photon number, which would be obtained from beam B alone, which has a mean time interval $2\Delta t_{\text{whole}}$ between arriving atoms. The two situations are not the same because in the microlaser the mean photon number does not vary linearly with the time interval.

As a first-order correction to the theory needed to account for the standing-wave structure, we assume that half of the atoms are located in planes along the nodes of the cavity and the remaining half are located in planes along the antinodes. Then only the atoms located in the antinode planes can interact with the cavity field, while the others pass through the cavity without interacting. This assumption is equivalent to counting only half of the atoms in the cavity. In fact, a second factor of two reduction in $\langle N \rangle$ occurs because of the Gaussian transverse profile of the cavity mode. Therefore, only one-quarter of the atoms in the apparent volume of the cavity are counted.

While $\langle N \rangle$ can be measured in the experiment, the pa-

parameter used in Eq. (7) is not $\langle N \rangle$ but rather the mean time interval Δt between successive arrivals, which is inversely proportional to $\langle N \rangle$. As shown below, these two parameters are related by

$$\langle N \rangle = \frac{t_{\text{int}}}{\sqrt{2}\Delta t}, \quad (11)$$

accounting for the standing-wave nature and the Gaussian profile of the cavity mode.

In order to explicitly show how the factor of one-quarter arises, consider an atomic beam of diameter $2R$ intersecting the cavity mode, as illustrated in Fig. 1. If $2R$ is smaller than the cavity length but much larger than the wavelength ($R \gg \lambda$), $\langle N \rangle$ can be calculated from the integral

$$\begin{aligned} \langle N \rangle &= n_0 \int_{-\infty}^{+\infty} dx \int_{-R}^R dy \exp \left[-2 \left(\frac{x^2 + y^2}{w_m^2} \right) \right] \\ &\quad \times \int_{-\sqrt{R^2 - y^2}}^{\sqrt{R^2 - y^2}} dz \cos^2 kz \\ &\cong n_0 w_m \sqrt{\frac{\pi}{2}} \int_{-R}^R dy \exp \left(-\frac{2y^2}{w_m^2} \right) \int_{-\sqrt{R^2 - y^2}}^{\sqrt{R^2 - y^2}} dz \frac{1}{2} \\ &= n_0 R^2 w_m \left(\frac{\pi}{2} \right)^{\frac{3}{2}} \eta(R/w_m), \end{aligned} \quad (12)$$

where n_0 is the density of the atomic beam, which can be measured independently in the experiment, and $\eta(\xi)$ is defined as

$$\eta(\xi) \equiv \frac{2}{\pi} \int_{-1}^1 dq \sqrt{1 - q^2} \exp(-2q^2 \xi^2). \quad (13)$$

Note the approximation in Eq. (12) that the standing-wave spatial variations are so rapid across the atomic beam that $\cos^2 kz \simeq 1/2$. The function $\eta(\xi)$ can be expressed in simple form in two limiting cases. When $R \ll w_m$,

$$\eta(R/w_m) \approx \frac{2}{\pi} \int_{-1}^1 dq \sqrt{1 - q^2} = 1, \quad (14)$$

and when $R \gg w_m$,

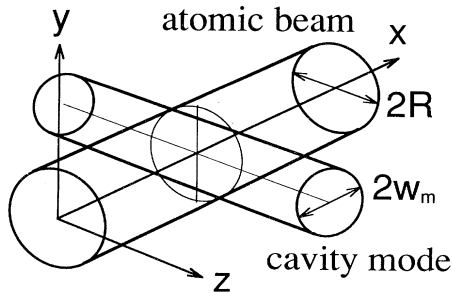


FIG. 1. Atomic beam intersecting the field mode of a high-order single-mode open optical resonator.

$$\eta(R/w_m) \approx \frac{2}{\pi} \int_{-1}^1 dq \exp[-2(R/w_m)^2 q^2] \approx \sqrt{\frac{2}{\pi}} \frac{w_m}{R}. \quad (15)$$

Therefore,

$$\langle N \rangle = \begin{cases} n_0 \frac{1}{4} \pi R^2 (2w_m) \sqrt{\frac{\pi}{2}} & \text{if } R \ll w_m \\ n_0 \frac{1}{4} \pi w_m^2 (2R) & \text{if } R \gg w_m. \end{cases} \quad (16)$$

The physical meaning of this result is as follows. When $R \gg w_m$, the averaging occurs over the $\cos^2 kz$ dependence, as well as over the Gaussian mode profile along x and y directions. Therefore, in order to obtain $\langle N \rangle$, the mean number of atoms in the apparent volume $\pi w_m^2 (2R)$ must be multiplied by an overall reduction factor

$$\frac{1}{2} \times \frac{1}{\sqrt{2}} \times \frac{1}{\sqrt{2}} = \frac{1}{4}.$$

On the other hand, if $R \ll w_m$ it is not necessary to average over y , so that the reduction factor is then

$$\frac{1}{2} \times \frac{1}{\sqrt{2}} = \frac{1}{2\sqrt{2}},$$

which is multiplied by an apparent volume of $\pi R^2 \sqrt{\pi} w_m$. Note that we have $\sqrt{\pi} w_m$ instead of $2w_m$ because of the Gaussian variation along the x direction.

In a similar way, the relation between $\langle N \rangle$ and Δt can be derived. For this, consider an infinitely narrow atomic beam ($R \ll w_m, \lambda$) traveling along one of the antinodes of the cavity. We assume that the mean time interval between atoms entering the cavity is Δt . The density is then simply

$$n_0 = \frac{1}{\pi R^2 v \Delta t}.$$

Since all the atoms are moving along the antinode,

$$\langle N \rangle = n_0 \frac{1}{\sqrt{2}} \pi R^2 \sqrt{\pi} w_m,$$

without the factor of $\frac{1}{2}$ (no averaging over z). Using the expression for the density, we then obtain

$$\langle N \rangle = \frac{1}{v \Delta t} \frac{1}{\sqrt{2}} \sqrt{\pi} w_m = \frac{\pi w_m / v}{\sqrt{2} \Delta t}. \quad (17)$$

We can generalize the result for \mathcal{N} infinitely narrow atomic beams traveling along the antinodes of the cavity. In this case the mean time interval becomes $\Delta t / \mathcal{N} \equiv \Delta t_{\text{whole}}$, but the result is the same as Eq. (17) except for Δt replaced with Δt_{whole} .

For a known value of $\langle N \rangle$, the mean time interval given by this equation can be used in the recursion relation Eq. (7). With this simple substitution, the y and z spatial dependences of the coupling constant are taken into account in an approximate way. For Gaussian mode functions the appropriate atom-field interaction time to be used is

$$t_{\text{int}} \equiv \frac{\sqrt{\pi} w_m}{v}. \quad (18)$$

Using this value of t_{int} , we can rewrite Eq. (17) in a simple form

$$\Delta t = \frac{t_{\text{int}}}{\sqrt{2} \langle N \rangle},$$

as stated in Eq. (11).

The principal data of the microlaser experiment of Ref. [1] are shown in Fig. 2. The curve denoted by “present theory” is obtained from the recursion relation Eq. (7) using Eqs. (16) and (11) to express the average number of atoms. This theory takes into account that a significant portion of the atoms entering the cavity are excited to superposition states in the microlaser, thereby inducing nonzero off-diagonal field matrix elements. It also incorporates the velocity distribution of the atomic beam [i.e., the results were averaged over this velocity distribution using Eq. (8)]. For comparison we also present the prediction of the micromaser theory of Ref. [5] (*micromaser theory*), for which the number of thermal photons was set equal to zero ($n_b = 0$) and the results were averaged over the velocity distribution. As mentioned above, the micromaser theory assumes that the off-diagonal elements of the field density operator all vanish.

The $\langle N \rangle$ values in Fig. 2 were obtained in Ref. [1] by measuring fluorescence in the cavity at 553 nm. The resulting values obtained for the number of atoms in the cavity were subject to a systematic uncertainty of about 50%. To fit the present theory best for small $\langle n \rangle$ and $\langle N \rangle$, the experimentally measured $\langle N \rangle$ values were all increased by 20%, well within the range of this systematic uncertainty. The open square in the figure denotes a data point before this scaleup with the horizontal error bar indicating the systematic uncertainty. Note that the curve predicted by micromaser theory is well outside the

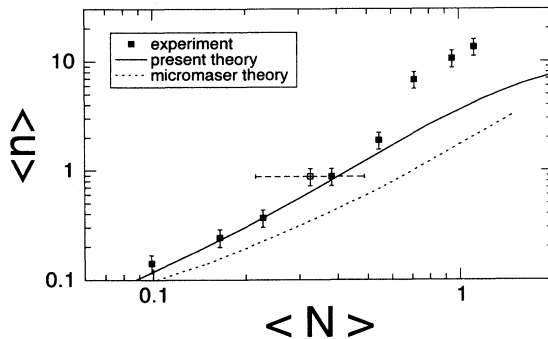


FIG. 2. Average number of photons in the cavity mode $\langle n \rangle$ as a function of the average number of atoms in the mode $\langle N \rangle$, as measured in Ref. [1] and predicted by various models. The horizontal error bar indicates a systematic uncertainty of 50% in $\langle N \rangle$ obtained in calibrating the number of atoms in the cavity by means of fluorescence. To fit the present theory best for small $\langle n \rangle$ and $\langle N \rangle$, the experimentally measured values of $\langle N \rangle$ were scaled up by 20%, well within this systematic uncertainty.

range of the systematic uncertainty.

The above scaleup procedure for fixing $\langle N \rangle$ gives good agreement between the data and the present theory when $\langle N \rangle$ and $\langle n \rangle$ are much less than one. However, when $\langle n \rangle$ becomes much larger than unity, the discrepancy between the data and the theory falls outside of the range of the systematic uncertainty of $\langle N \rangle$. The experimental results clearly indicate a rapid change in the slope near $\langle N \rangle \simeq 0.6$, well before the single-atom interaction approximation becomes invalid (the probability for more than one atom is 13% for $\langle N \rangle = 0.6$). This rapid rise can be explained by the standing-wave nature of the cavity mode, as described above. In reality, atoms are distributed throughout the standing-wave structure of the cavity mode, those near the antinodes experiencing maximum coupling strength, whereas those near the nodes experience no coupling at all. The above calculation makes the simplifying assumption that half of the atoms are at the nodes, with the remaining half at the antinodes. This is a good approximation as long as the number of photons in the cavity mode is relatively small, as confirmed by the good agreement with the experimental data. However, the approximation breaks down when the photon number begins to grow large. In that case, even the atoms near the nodes can interact with the cavity field, mostly generated by atoms traveling near the antinodes. For atoms near the nodes, even though coupling is reduced by the $\cos kz$ function, the Rabi frequency that governs photon emission from the atoms is increased by the factor $\sqrt{n+1}$, with photon number n much larger than one. Accordingly, except for the atoms traveling exactly along the nodes, essentially all of the atoms can participate in the photon emission process. The upper bound of $\langle n \rangle$ caused by this saturation effect should be what we would find if the coupling did not vary sinusoidally along the cavity axis and if all the atoms assumed the full strength of the coupling constant. In this case the number of atoms contributing to laser oscillation is simply doubled. In Fig. 3 the experimental data are compared with the curve indicating the upper bound of the output power, based on this argument. Note that in our data the rapid change in slope occurs when $\langle n \rangle \sim 3$, which is certainly large enough for the onset of the saturation effect. This upper bound ar-

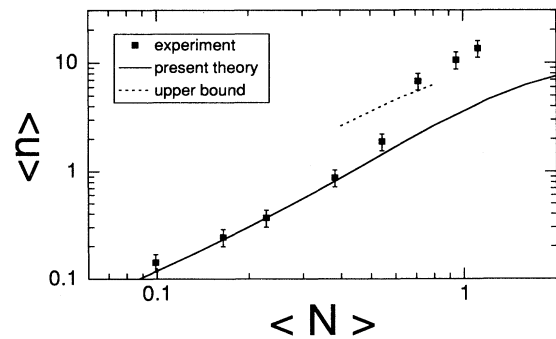


FIG. 3. Experimental data of Ref. [1] plotted again in comparison with the curve indicating the upper bound of the output power, based on the discussion in the text.

gument hence gives insight into the rapid increase in $\langle n \rangle$. There still exists a discrepancy between the data and the theory when $\langle N \rangle \approx 1$. In this case an effective number of atoms contributing to laser oscillation N_{eff} can be as large as twice $\langle N \rangle$, since saturation is fully effective. We suspect that the discrepancy occurs since more than one atom interacts simultaneously with the cavity field with significant probability ($\sim 60\%$ for $N_{\text{eff}} \approx 2$), invalidating the present one-atom quantum theory. Few quantum mechanical treatments of the micromaser with a few atoms in the cavity have appeared [14,15] and a complete theory is yet to be developed.

IV. CONCLUSION

An approximate treatment of the standing-wave character of the cavity has been presented to explain the size of the observed microlaser signal. Using the fully quantum mechanical microlaser theory, the standing-wave nature of the microlaser cavity mode has been accounted for in an approximate way and an upper bound to the mean photon number has been estimated to explain the observed rapid increase in signal in the large photon number limit. A rigorous approach would entail solving the quantum mechanical master equation, including the standing-wave character, and allowing more than one atom to reside in the cavity. Such a solution would be extremely complex. Alternatively, one can employ numerical simulations, particularly ones based on the Monte Carlo wavefunction method [16]. In this type of simulation, the time-dependent solution must be followed for a long sequence of atom-field interactions, with random atomic positions at each interaction. This result is expected to approach the actual solution gradually after a large number of interactions.

ACKNOWLEDGMENTS

We thank Ramachandra R. Dasari and James J. Childs for many helpful discussions. This work is supported by NSF Grants Nos. PHY-9112421 and CHE-9304251.

APPENDIX: DERIVATION OF EQ. (7)

The derivation presented here is a generalization of the relevant part of the micromaser theory of Ref. [5]. Consider a microlaser system in which the i th atom enters the cavity at $t = t_i$, the next atom at $t = t_{i+1}$, and so on. Then for $t_i + t_{\text{int}} < t < t_{i+1}$, the system is described

by Eq. (3). We define an operator L

$$\frac{d\rho^F}{dt} = \frac{\Gamma_c}{2} (2a\rho^F a^\dagger - a^\dagger a \rho^F - \rho^F a^\dagger a) \equiv L\rho^F. \quad (\text{A1})$$

Then, formally,

$$\rho^F(t_{i+1}) = \exp(t_p L) \rho^F(t_i + t_{\text{int}}), \quad (\text{A2})$$

where $t_p \equiv t_{i+1} - (t_i + t_{\text{int}})$. Assuming that the time interval between two successive atoms conforms to a Poissonian distribution given by

$$f(t_p) = \frac{1}{\Delta t} \exp\left[-\frac{t_p + t_{\text{int}}}{\Delta t}\right] \quad (\text{A3})$$

and averaging Eq. (A2) over the distribution, we obtain

$$\begin{aligned} \langle \rho^F(t_{i+1}) \rangle &\equiv \int_0^\infty \rho^F(t_{i+1}) f(t_p) dt_p \\ &= \langle \exp(t_p L) \rangle \langle \rho^F(t_i + t_{\text{int}}) \rangle \\ &= \frac{\exp(-\frac{t_{\text{int}}}{\Delta t})}{1 - \Delta t L} \langle \rho^F(t_i + t_{\text{int}}) \rangle, \end{aligned} \quad (\text{A4})$$

where we assume the arrival time of the i th atom to be statistically independent from that of the $(i+1)$ th atom. The exponential factor $\exp(-t_{\text{int}}/\Delta t)$ arises because cavity damping is neglected during the time interval $t_i < t < t_i + t_{\text{int}}$. The cavity damping during that time interval can be approximately accounted for in the model by modification of Eq. (A2) to

$$\rho^F(t_{i+1}) \approx \exp[(t_{i+1} - t_i)L] \rho^F(t_i + t_{\text{int}}), \quad (\text{A5})$$

which results in neglecting the exponential factor in Eq. (A4). Invoking a boundary condition that ρ^F repeats the same time evolution for every atom once, an equilibrium is reached:

$$\langle \rho^F(t_{i+1}) \rangle_{\text{eq}} = \langle \rho^F(t_i) \rangle_{\text{eq}} \quad \text{for any } i, \quad (\text{A6})$$

and denoting the matrix element of $\langle \rho^F(t) \rangle_{\text{eq}}$ as $Q_{n,m}(t)$, we then obtain

$$Q_{n,m}(0) - \Delta t L Q_{n,m}(\Delta t) = Q_{n,m}(t_{\text{int}}), \quad (\text{A7})$$

which, by the definition of the L operator, reduces to

$$Q_{n,m}(0) - \Delta t \left. \frac{dQ_{n,m}(t)}{dt} \right|_{t=\Delta t} = Q_{n,m}(t_{\text{int}}). \quad (\text{A8})$$

Averaging Eq. (4) over the Poissonian distribution for random arrivals of atoms then gives

$$\begin{aligned} Q_{n,m}(t) &= Q_{n,m}(0) \{ \rho_{aa}^A [C_n(t)C_m(t) + S_n^\delta(t)S_m^\delta(t) - i[C_n(t)S_m^\delta(t) - C_m(t)S_n^\delta(t)]] \\ &\quad + \rho_{bb}^A [C_{n-1}(t)C_{m-1}(t) + S_{n-1}^\delta(t)S_{m-1}^\delta(t) + i[C_{n-1}(t)S_{m-1}^\delta(t) - C_{m-1}(t)S_{n-1}^\delta(t)]] \} \\ &\quad + Q_{n+1,m+1}(0) \rho_{bb}^A S_n^\kappa(t) S_m^\kappa(t) + Q_{n-1,m-1}(0) \rho_{aa}^A S_{n-1}^\kappa(t) S_{m-1}^\kappa(t) \\ &\quad + iQ_{n,m+1}(0) \rho_{ab}^A [C_n(t) + iS_n^\delta(t)] S_m^\kappa(t) - iQ_{n+1,m}(0) \rho_{ba}^A S_n^\kappa(t) [C_m(t) - iS_m^\delta(t)] \\ &\quad + iQ_{n,m-1}(0) \rho_{ba}^A [C_{n-1}(t) - iS_{n-1}^\delta(t)] S_{m-1}^\kappa(t) - iQ_{n-1,m}(0) \rho_{ab}^A S_{n-1}^\kappa(t) [C_{m-1}(t) + iS_{m-1}^\delta(t)] \end{aligned} \quad (\text{A9})$$

for $0 \leq t \leq t_{\text{int}}$. Similarly, from Eq. (6),

$$\frac{dQ_{n,m}}{dt} = \Gamma_c \left[\sqrt{(n+1)(m+1)} Q_{n+1,m+1} - \frac{1}{2}(n+m) Q_{n,m} \right] \quad (\text{A10})$$

for $t_{\text{int}} \leq t \leq \Delta t$. Evaluating Eq. (A9) at $t = t_{\text{int}}$ and Eq. (A10) at $t = \Delta t$ (or equivalently at $t = 0$) and substituting the results into Eq. (A8), we then obtain

$$\begin{aligned} Q_{n,m} - \Delta t \Gamma_c \left[\sqrt{(n+1)(m+1)} Q_{n+1,m+1} - \frac{1}{2}(n+m) Q_{n,m} \right] \\ = Q_{n,m} \{ \rho_{aa}^A [C_n C_m + S_n^\delta S_m^\delta - i(C_n S_m^\delta - C_m S_n^\delta)] \\ + \rho_{bb}^A [C_{n-1} C_{m-1} + S_{n-1}^\delta S_{m-1}^\delta + i(C_{n-1} S_{m-1}^\delta - C_{m-1} S_{n-1}^\delta)] \} \\ + Q_{n+1,m+1} \rho_{bb}^A S_n^\kappa S_m^\kappa + Q_{n-1,m-1} \rho_{aa}^A S_{n-1}^\kappa S_{m-1}^\kappa \\ + i Q_{n,m+1} \rho_{ab}^A (C_n + i S_n^\delta) S_m^\kappa - i Q_{n+1,m} \rho_{ba}^A S_n^\kappa (C_m - i S_m^\delta) \\ + i Q_{n,m-1} \rho_{ba}^A (C_{n-1} - i S_{n-1}^\delta) S_{m-1}^\kappa - i Q_{n-1,m} \rho_{ab}^A S_{n-1}^\kappa (C_{m-1} + i S_{m-1}^\delta) , \end{aligned} \quad (\text{A11})$$

which is identical to Eq. (7) of the main text. Here $Q_{n,m}$, C_n , S_n^κ , and S_n^δ are shorthand notations for $Q_{n,m}(0)$, $C_n(t_{\text{int}})$, $S_n^\kappa(t_{\text{int}})$, and $S_n^\delta(t_{\text{int}})$, respectively.

- [1] Kyungwon An, James J. Child, Ramachandra R. Dasari, and Michael S. Feld, *Phys. Rev. Lett.* **73**, 3375 (1994).
- [2] *Cavity Quantum Electrodynamics*, edited by P. Berman (Academic, New York, 1993).
- [3] S. Haroche and D. Kleppner, *Phys. Today* **42** (1), 24 (1989).
- [4] D. Meschede, H. Walther, and G. Müller, *Phys. Rev. Lett.* **54**, 551 (1985).
- [5] P. Filipowicz, J. Javanainen, and P. Meystre, *Phys. Rev. A* **34**, 3077 (1986).
- [6] E. T. Jaynes and F. W. Cummings, *Proc. IEEE* **51**, 89 (1963).
- [7] S. Qamar and M. S. Zubairy, *Phys. Rev. A* **44**, 7804 (1991).
- [8] M. O. Scully, H. Walther, G. S. Agarwal, T. Quang, and W. Schleich, *Phys. Rev. A* **44**, 5992 (1991).
- [9] T. Quang, G. S. Agarwal, J. Bergou, M. O. Scully, and H. Walther, *Phys. Rev. A* **48**, 803 (1993).
- [10] K. Vogel, W. P. Schleich, M. O. Scully, and H. Walther, *Phys. Rev. A* **48**, 813 (1993).
- [11] The quantum collapse and revival has been demonstrated in the micromaser in the presence of blackbody radiation. See G. Rempe, H. Walther, and N. Klein, *Phys. Rev. Lett.* **58**, 353 (1987).
- [12] P. Filipowicz, J. Javanainen, and P. Meystre, *J. Opt. Soc. Am. B* **3**, 906 (1986).
- [13] P. Meystre, G. Rempe, and H. Walther, *Opt. Lett.* **13**, 1078 (1988).
- [14] M. Orszag and R. Ramirez, *Phys. Rev. A* **49**, 2933 (1994).
- [15] Edda Wehner, Raffaella Seno, Nicoletta Sterpi, Berthold-Georg Englert, and Herbert Walther, *Opt. Commun.* **110**, 655 (1994).
- [16] For example, see L. Tian and H. J. Carmichael, *Phys. Rev. A* **46**, R6801 (1992); H. J. Carmichael, *Phys. Rev. Lett.* **70**, 2273 (1993); R. Dum, P. Zoller, and H. Ritsch, *Phys. Rev. A* **45**, 4879 (1992); R. Dum, A. S. Parkins, P. Zoller, and C. W. Gardiner, *ibid.* **46**, 4382 (1992); P. Marte, R. Dum, R. Taieb, P. D. Lett, and P. Zoller, *Phys. Rev. Lett.* **71**, 1335 (1993).